

Electronic spectral shift of oxygen-filled (6,6) carbon nanotubes

Hiroyuki Shima^{a,*}, Hideo Yoshioka^b

^a*Division of Applied Physics, Faculty of Engineering, Hokkaido University, Sapporo, Hokkaido 060-8628, Japan*

^b*Department of Physics, Nara Women's University, Nara 630-8506, Japan*

Abstract

Electronic state modulation of the armchair (6,6) carbon nanotubes filled with a linear assembly of oxygen molecules is addressed theoretically. Ferromagnetic coupling of encapsulated oxygen produces a magnetic field with cylindrical symmetry, which deviates the electron's eigenenergies from those prior to the oxygen absorption. An intriguing spectral gap arises near the Fermi energy, at which the gap formation is allowed only when the tube length equals to a multiple of three in units of carbon hexagon. A possible means to detect the selective gap formation is discussed.

Keywords: Armchair carbon nanotube, gas absorption, HOMO-LUMO gap, ferromagnetic chain

1. Introduction

The central cavity of carbon nanotubes is an ideal container for atoms and small molecules. Initiated by the massive H₂-storage observation [1], many attempts to introduce foreign entities into the hollow space of nanotubes have been reported: H₂O [2, 3, 4], H₂O₂ [5], CO₂ [6], C₂H₂ [7], and Ar[8] are only a few to mention. In addition to the potential utility for energy-storage materials and molecular transport devices, the filling of carbon nanotubes is believed to open up novel applications of drug delivery to the cell [5, 9, 10]. In light to mechanical flexibility of nanotubes [11], furthermore, effects of their cross-sectional deformation on the properties of the encapsulated molecules have also been suggested [12, 13].

Among many kinds of intercalates, special attention has to be paid for dioxygen molecules (O₂) confined into single-walled carbon nanotubes (SWNTs). An O₂ molecule is the best known realization of a *p*-electron magnetic material; it has two unpaired electrons in a doubly degenerate antibonding orbital, thus being a spin $S = 1$ magnet in the ground state. In the bulk solid state, O₂ assembly often exhibits anti-ferromagnetic ordering with mutually parallel arrangement [14, 15]. But confinement into thin long cavity can lead ferromagnetic couplings of adjacent O₂ molecules, in which the O-O bond orientations of two entities are orthogonal to each other [16, 17]. In fact, the ferromagnetic ordering of a one-dimensional O₂ chain is available through confinement into an armchair SWNT of the (6,6) chirality, as evidenced by molecular dynamics simulations [18]. Structural control of such magnetic molecular aggregates is attractive in view of low-dimensional physicochemistry, and thus attempts based on various host materials have been made to stabilize the ferromagnetic order of absorbed O₂ molecules [19, 20].

A possible consequence of the ferromagnetic O₂ molecular chain inside a SWNT is that the resulting magnetic field affects

electronic properties of the host SWNT. Magnetic field application in general breaks time-reversal symmetry of the system. This symmetry breaking can lead feasible field-induced phenomena such as the Aharonov-Bohm effect [21, 22] and the Landau level splitting [23] depending on the field strength and direction. Particularly in the O₂-filled (6,6) SWNT, encapsulated O₂ molecules are extremely close to the surrounding carbon layer; therefore, their magnetic moments are thought to yield significant alteration in the quantum states of π electrons, which has remained unsettled so far.

In this work, we theoretically investigate the electronic structures of finite-length armchair (6,6) SWNTs encapsulating the ferromagnetic O₂ chain. Spectral shifts caused by the O₂ absorption are found to be strongly dependent both on the tube length and the energy region to be studied. A signature of the O₂ chain confinement manifests in the field-induced gap at the Fermi energy. Interestingly, the gap arises only when the tube length equals to a multiple of three in units of carbon hexagon, while it vanishes other tube lengths. This length-dependent gap formation may be observed in the electronic response of the O₂-filled nanotubes to alternate voltage with tens gigahertz frequency.

2. Model and Methods

2.1. Hamiltonian

We consider the electronic structure of O₂-filled (6,6) SWNTs utilizing the nearest-neighbor tight-binding model. The host graphitic sheet is the one rolled up in the direction of a C-C bond with the bond length of $a_{C-C} = 0.142$ nm, having a structural periodicity of the lattice constant of $a = \sqrt{3}a_{C-C} = 0.246$ nm along the tube axis. The tube length L is thus written by $N_y a$, where N_y is the number of hexagons aligned in the axial direction. Accordingly, $12N_y$ hexagons composed of $24(N_y + 1) [= N_C]$ carbon atoms are involved in the system. The

*Corresponding Author: shima@eng.hokudai.ac.jp

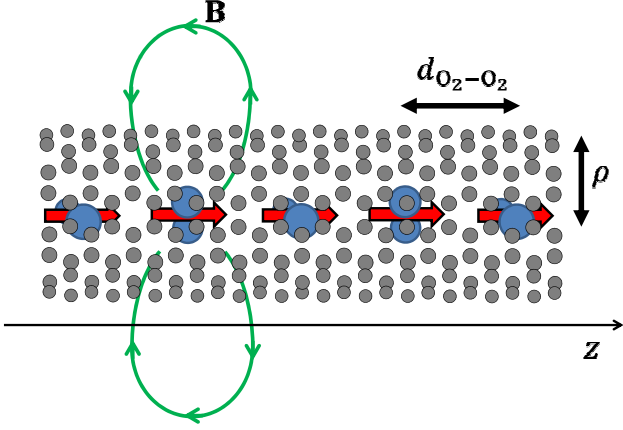


Figure 1: Schematic of the O₂-filled armchair (6,6) SWNT with the tube radius $\rho = 0.407$ nm. Small (colored in gray) and large (blue) circles are the constituent atoms of carbon and oxygen, respectively. Thick arrows indicate the magnetic dipole moments μ_{O_2} associated with the unpaired electrons in O₂ molecules, which align with a separation $d_{O_2-O_2} = 0.33$ nm. The magnetic field profile \mathbf{B} generated by single O₂ molecule is depicted by curved paths.

dangling bonds at the tube edges are assumed to be passivated by hydrogen atoms.

The Hamiltonian matrix is built from the subspace spanned by the N_C wave functions of $2p_z$ orbitals. The nearest-neighbor Hamiltonian is given by $\hat{\mathcal{H}} = \sum_{i,j} \gamma_{i,j} \hat{c}_i^\dagger \hat{c}_j$, where $\gamma_{i,j}$ is the transfer energy between the nearest-neighbor sites, and \hat{c}_i^\dagger (\hat{c}_i) is the creation (annihilation) operator of the π electron at the site i . The electronic states are obtained by diagonalizing the $N_C \times N_C$ Hermitian matrix. When the system is subjected to a magnetic field, the transfer integral $\gamma_{i,j}$ becomes $\gamma_{i,j} = \gamma_0 e^{2\pi i \phi_{i,j}}$ with $\gamma_0 = 2.7$ eV, where $\phi_{i,j} = (e/h) \int_{\mathbf{r}_i}^{\mathbf{r}_j} \mathbf{A} \cdot d\mathbf{l}$ is the Peierls phase and \mathbf{A} is the vector potential corresponding to the magnetic field. In the present system, the ferromagnetic O₂ chain produces a spatially modulated magnetic field, and the magnetic flux passing through each carbon hexagonal ring provides a finite value of $\phi_{i,j}$ at edges of the hexagon.

2.2. Magnetic field distribution

The stable magnetic spin ($S = 1$) in an isolated O₂ molecule generates the magnetic field \mathbf{B}_{O_2} at a point $\mathbf{r} = \rho \mathbf{e}_\rho + z \mathbf{e}_z$ in terms of the cylindrical polar coordinates (ρ, θ, z) . The induced magnetic field is written by

$$\mathbf{B}_{O_2}(\mathbf{r}) = \frac{\mu_0}{4\pi} \frac{3\mathbf{r}(\mathbf{r} \cdot \boldsymbol{\mu}_{O_2}) - r^2 \boldsymbol{\mu}_{O_2}}{r^5}, \quad (1)$$

where $\boldsymbol{\mu}_{O_2} = -g_e \mu_B \mathbf{S} / \hbar$ with $g_e = 2$, $\mathbf{S} = \hbar \mathbf{e}_z$, and $\mu_B = e\hbar/(2m_e)$; e and m_e are the bare electron's charge and mass, respectively, and μ_0 is the permeability of vacuum. Our task is to evaluate the normal component of \mathbf{B}_{O_2} , given by $B_\perp = \mathbf{B}_{O_2} \cdot \mathbf{e}_\rho$, which exerts just on the graphitic sheet. Using the relations of $\boldsymbol{\mu}_{O_2} \cdot \mathbf{e}_\rho = 0$ and $\mathbf{r} \cdot \mathbf{e}_\rho = \rho$ with ρ being the tube radius, the sum of the normal components, $B_\perp^{\text{all}}(z)$, associated with all O₂ molecules

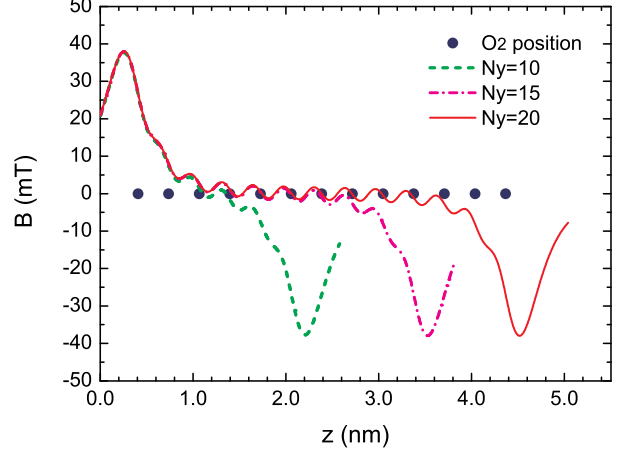


Figure 2: Spatial distribution of the normal component B_\perp^{all} of the magnetic field caused by the O₂ molecular chain in the hollow cavity of (6,6) SWNTs.

encapsulated in the (6,6) tube is given by

$$B_\perp^{\text{all}}(z) = \frac{-3\mu_0\mu_B}{2\pi} \sum_{n=1}^{N_{O_2}} \frac{\rho(z - \rho - nd_{O_2-O_2})}{[\rho^2 + (z - \rho - nd_{O_2-O_2})^2]^{5/2}}. \quad (2)$$

Here, $d_{O_2-O_2} = 0.33$ nm is the separation between adjacent O₂ molecules [18], and N_{O_2} is the total number of the O₂ molecules that position at $z \in [\rho, L - \rho]$ with equiseperation. We set $\rho = 0.407$ nm according to the formula $\rho = a \sqrt{n^2 + m^2 + nm} / (2\pi)$ for nanotubes with (n, m) chirality. As a result, the magnetic flux $\Phi(z)$ that penetrates a hexagonal plaquette at z reads as $\Phi(z) = \sqrt{3} B_\perp^{\text{all}} a^2 / 2$, and the Peierls phase $\phi_{i,j}$ can be determined via the relation $\sum_{\text{hexagon}} \phi_{i,j} = \Phi(z) / \Phi_0$ with $\Phi_0 = h/e$ being flux quantum.

Figure 2 illustrates the spatial distribution of $B_\perp^{\text{all}}(z)$ for several tube lengths expressed by N_y . Solid circles indicate the position of O₂ molecules that may be contained in the host nanotube. In the $N_y = 10$ case, for instance, the six O₂ to the most left (*i.e.*, up to the O₂ at $z = 2.06$ nm) can be included within the allowed region of $z \in [\rho, L - \rho]$ so that $N_{O_2} = 6$. Similarly, $N_{O_2} = 10, 13$ for $N_y = 15, 20$, respectively. We observe that $B_\perp^{\text{all}}(z)$ oscillates with a slight amplitude in-between region but exhibits a large amplitude on the order of 20 mT near the tube edges. The amplitude suppression at the intermediate region is attributed to cancelling out the oppositely-oriented field components associated with O₂ molecules separated by ~ 1 nm each other. Neighborhoods of the tube edges are free from the suppression due to the absence of O₂ both at $z < \rho$ and $z > L - \rho$, and thus significant amount of the Peierls phase is imposed locally to the electron's eigenmodes. As the scenario holds regardless of the tube length, the electronic states for longer (6,6) SWNTs are modulated to a degree by the O₂ absorption, despite of slight magnetic moments of individual O₂ molecules.

3. Results

Figure 3 displays the O₂-induced shift in the electronic energy spectra of short (6,6) SWNTs. The tube length is set to

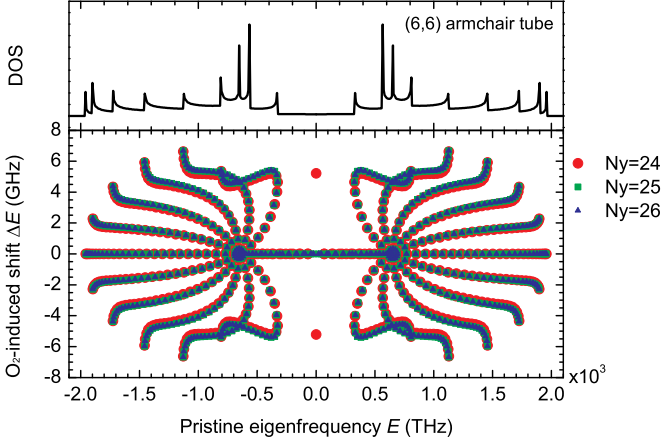


Figure 3: Top: Spectral density of states of an empty (*i.e.*, O₂-unfilled) (6,6) nanotube. Bottom: O₂-induced spectral shift for several tube lengths measured by N_y .

be $N_y = 24, 25, 26$ as simple examples, while much longer nanotubes yield similar results as those in this plot. The horizontal axis E represents the eigenenergies of the pristine system (*i.e.*, prior to O₂ absorption), and the vertical axis ΔE gives their shifts caused by O₂ absorption. Each discrete point in the plot indicates the quantum states of isolated finite-length (6,6) SWNTs, which are written by standing waves of the form $\psi_n(z) \propto \sin(k_n z)$ with a discrete set of wavenumbers $k_n = n\pi/(N_y a)$ where $n = 1, 2, \dots, N_y$ [24]. If the O₂ chain were absent, $\Delta E \equiv 0$ so that N_C discrete points would be line up horizontally in the bottom panel of Fig. 3. But in the current system, the O₂-induced magnetic field modulates the π electron states, which results in upward or downward shift in the eigenenergies as quantified by ΔE in the figure.

The data in Fig. 3 show pronounced shifts from the pristine values at discrete energies that correspond to the van Hove singularities of the spectral density of states (top panel). A marked exception is the anomalous point-like shift at the band center ($E = E_F = 0$), which arises only in the case of $N_y = 24$. This point-like energy shift implies an energy-gap formation between the highest occupied state and the lowest unoccupied state in the vicinity of $E = 0$. It should be emphasized that the energy gap no longer disappears in the other two cases of $N_y = 25, 26$ as clarified visually in Inset of Fig. 4.

We have revealed that the O₂-induced energy gap mentioned above is universally observed every when $\text{mod}(N_y, 3) = 0$. Figure 4 presents the N_y dependence of the gap magnitude E_g ; Note that only E_g at $N_y = 3, 6, 9, \dots$ are plotted, because $E_g = 0$ whenever $\text{mod}(N_y, 3) \neq 0$. The result exhibits a monotonic increase with N_y followed by a convergence in the large N_y limit with the asymptotic value of $E_g \sim 13.6$ GHz. We mention that $N_y = 201$ corresponds to the tube length ~ 60 nm, which scale is in a realm of the current fabrication techniques. It also follows from Fig. 4 that the Zeeman splitting is irrelevant to the gap formation, since the energy scale $\mu_B B$ in the present condition is on the order of 0.1 GHz, far less than the gap magnitude.

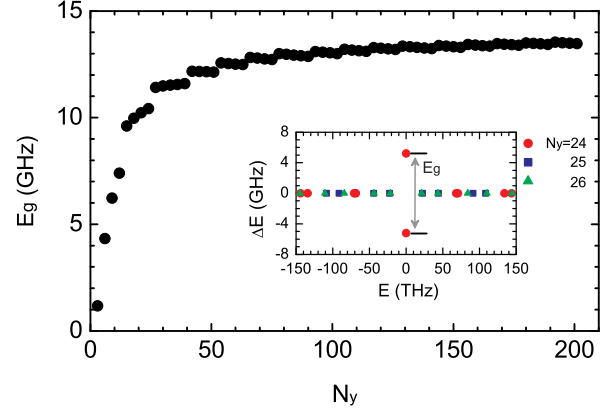


Figure 4: HOMO-LUMO energy gap E_g as a function of the tube length N_y . E_g grows monotonically with increasing N_y and converges to ~ 13.6 GHz in the large N_y limit. Inset: Enlarged view of the O₂-induced eigenenergy shift in the vicinity of $E = 0$.

4. Discussion

The length-dependent gap formation at the Fermi level is understood by considering the eigenlevel configuration for different N_y . The left panel in Fig. 5 shows the energy dispersion relation for the infinitely-long (6,6) nanotube free from the ferromagnetic O₂ chain. There are fourteen branches reflecting the quantum confinement effect on the π electrons along the circumferential direction. Of these branches, ten thick curves are doubly-degenerate at every k points, while four thin curves are non-degenerate except for the crossing point at $k = k_F = 2\pi/(3a)$. All the degeneracy is lifted when the ferromagnetic O₂ chain is built inside the SWNT; it then leads the spectral shifts of all initially-degenerate eigenmodes that lie along the ten thick branches, which have been already demonstrated in the bottom panel of Fig. 3.

The abovementioned scenario holds for finite-length (6,6) nanotubes, while the discreteness of allowed wavenumbers in the axial direction requires subtle modification. The right panel of Fig. 5 gives a drawing of the level configuration for N_y -long O₂-free (6,6) nanotubes in the vicinity of $E = 0$. Solid circles indicate the eigenlevels for N_y such that $\text{mod}(N_y, 3) = 0$, and square ones for $\text{mod}(N_y, 3) \neq 0$. In the former case, only one doubly-degenerate state (indicated by a large solid circle) resides just on the crossing point. In contrast, the latter case involves no degenerate state. Upon the O₂ chain encapsulation, therefore, the degeneracy removal arises only in the N_y -long nanotubes with $\text{mod}(N_y, 3) = 0$. This mechanism accounts for the length-sensitive gap formation at the Fermi level.

The degeneracy at the crossing point owes the availability of an appropriate value of the discrete wavenumber $k_n = n\Delta k$ with interval $\Delta k = \pi/(N_y a)$. When $N_y = 3\ell$ with integer ℓ , the interval reads $\Delta k = \pi/(3\ell a)$ and thus the discrete set of k_n can take the value of the Fermi wavenumber $k_F = 2\pi/(3a)$ at $n = 2\ell$. But when $N_y \neq 3\ell$, the resulting interval $\Delta k' = \pi/[(3\ell \pm 1)a]$ forbids any k_n to coincides with k_F since there is no integer n such that $n/(3\ell \pm 1) = 2/3$.

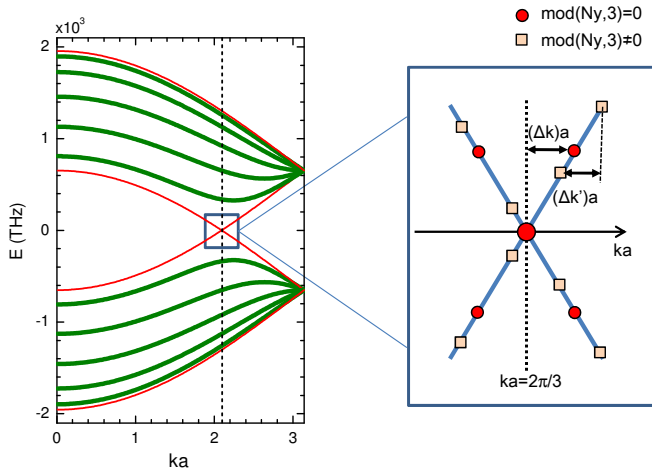


Figure 5: Left: Energy dispersion relation for armchair (6,6) nanotubes free from the ferromagnetic O₂ chain. Ten thick curves are doubly-degenerate at every k points, while four thin curves are non-degenerate except for the crossing point at $k = k_F = 2\pi/(3a)$. Right: Eigenlevel configuration of an empty nanotube near the Fermi energy $E_F = 0$. Only when $\text{mod}(N_y, 3) = 0$, a doubly-degenerate state (indicated by a large solid circle) resides just on the crossing point.

We suggest that the O₂-induced gap with the magnitude of 13.6 GHz can be detected through the dynamical conductivity measurement at low temperature. According to the Kubo formula [25, 26], the dynamical conductance along the tube axis is found as

$$G(\omega) = -\frac{1}{i\omega} \sum_{\mu, \nu} |J_{\mu\nu}^z|^2 \frac{f_\mu - f_\nu}{\hbar\omega + E_\mu - E_\nu + i\delta}, \quad (3)$$

where f_μ and f_ν are Fermi distribution functions and δ is positive infinitesimal. The magnitude of $G(\omega)$ is primarily determined by $J_{\mu\nu}^z = \langle E_\mu | \hat{J}_z | E_\nu \rangle$, in which \hat{J}_z is the z component of the current operator $\hat{\mathbf{J}} = (-ie/\hbar)[\hat{\mathbf{r}}, \hat{H}]$ with a commutator $[\hat{\cdot}, \hat{\cdot}]$. Suppose that ac electric voltage with frequency ω is applied to the O₂-filled nanotubes. A sufficiently low temperature of $k_B T \leq \hbar\omega$, Eq. (3) is reduced to $G(\omega) \propto |J_{+-}|^2/\omega$, where $J_{+-} = \langle E_+ | \hat{J}_z | E_- \rangle$ and $E_{+(-)}$ is the eigenlevel immediately above (below) $E_F = 0$. In the present system, J_{+-} has a modestly large value, which follows from the numerical result of $|\sum_{i=1}^{N_C} \langle E_+ | \mathbf{r}_i \rangle \langle \mathbf{r}_i + \mathbf{e}_z | E_- \rangle| \sim 0.2$ under the normalization condition of $\sum_{i=1}^{N_C} |\langle \mathbf{r}_i | E_{+(-)} \rangle|^2 = 1$. Hence, the dynamical conductivity will exhibit a sharp peak at $\omega \sim 13.6$ GHz in a low-temperature measurement at less than 1 K. A large-scale computation technique for the Kubo-formula [27, 28] incorporated with *ab initio* calculations [29] enable a quantitative examination of the conjecture, which we will perform in the future work.

5. Summary

We have theoretically considered the electronic spectral shift of the (6,6) SWNT encapsulating a linear ferromagnetic O₂ chain into the hollow cavity. O₂ absorption causes an energy gap between the highest and lowest occupied states only in the

N_y -long (6,6) SWNTs with N_y being multiples of three; the gap vanishes for other N_y . The length-sensitive gap formation is attributed to the removal of eigenlevel degeneracy at the Fermi level that arises only when $\text{mod}(N_y, 3) = 0$. The gap magnitude approaches 13.6 GHz in the long- N_y limit, which suggests the possibility that the O₂-induced gap can be confirmed in the alternative-current measurement of the host SWNT.

Acknowledgment

Fruitful discussion with H. Suzuura is greatly acknowledged. This work was supported by MEXT and Nara Women's University Intramural Grant for Project Research. HS cordially thanks the financial supports by the Inamori Foundation and the Suhara Memorial Foundation.

References

- [1] A. C. Dillon, K. M. Jones, T. A. Bekkedahl, C. H. Kiang, D. S. Bethune, M. J. Heben, *Nature* 386 (1997) 377.
- [2] M. C. Gordillo, J. Martí, *Chem. Phys. Lett.* 329 (2000) 341.
- [3] Y. Maniwa, H. Kataura, M. Abe, A. Uda, S. Suzuki, Y. Achiba, H. Kira, K. Matsuda, H. Kadowaki and Y. Okabe, *Chem. Phys. Lett.* 401 (2005) 534.
- [4] A. Alexiadis, S. Kassinos, *Chem. Rev.* 108 (2008) 5014.
- [5] C. N. Ramachandran, D. D. Fazio, N. Sathiyamurthy, V. Aquilanti, *Chem. Phys. Lett.* 473 (2009) 146.
- [6] A. Alexiadis and S. Kassinos, *Chem. Phys. Lett.* 460 (2008) 512.
- [7] G. Kim, Y. Kim and J. Ihm, *Chem. Phys. Lett.* 415 (2005) 279.
- [8] G. E. Gadd, M. Blackford, S. Moricca, N. Webb, P. J. Evans, A. M. Smith, G. Jacobsen, S. Leung, A. Day and Q. Hua, *Science* 277 (1997) 933.
- [9] T. A. Hilder, J. M. Hill, *Nanotechnology* 18 (2007) 275704.
- [10] Z. Liu, S. Tabakman, K. Welscher, H. Dai, *Nano Res.* 2 (2009) 85.
- [11] H. Shima, M. Sato, *Elastic and Plastic Deformation of Carbon Nanotubes*, Pan Stanford Publishing, Singapore (2011).
- [12] H. Shima, M. Sato, *Nanotechnology* 19 (2008) 495705.
- [13] H. Shima, M. Sato, K. Iibishi, S. Ghosh, M. Arroyo, *Phys. Rev. B* 82 (2010) 085401.
- [14] Y. A. Freiman, H. J. Jodl, *Phys. Rep.* 401 (2004) 1.
- [15] S. Klotz, T. Strässle, A. L. Cornelius, J. Philippe, T. Hansen, *Phys. Rev. Lett.* 104 (2010) 115501.
- [16] M. C. van Hemert, P. E. S. Wormer, A. van der Avoird, *Phys. Rev. Lett.* 51 (1983) 1167.
- [17] B. Bussery, P. E. S. Wormer, *J. Chem. Phys.* 99 (1993) 1230.
- [18] K. Hanami, T. Umesaki, K. Matsuda, Y. Miyata, H. Kataura, Y. Okabe, Y. Maniwa, *J. Phys. Soc. Jpn.* 79 (2010) 023601.
- [19] S. Takamizawa, E. Nakata, T. Akatsuka, C. Kachi-Terajima, R. Miyake, *J. Am. Chem. Soc.* 130 (2008) 17882.
- [20] S. Riyadi, S. Giriapura, R. A. de Groot, A. Caretta, P. H. M. van Loosdrecht, T. T. M. Palstra, G. R. Blake, *Chem. Mater.* 23 (2011) 1578.
- [21] H. Ajiki, T. Ando, *J. Phys. Soc. Jpn.* 62 (1993) 2470.
- [22] A. Bachtold, C. Strunk, J. P. Salvetat, J. M. Bonard, L. Forró, T. Nussbaumer, C. Schönenberger, *Nature* 397 (1999) 673.
- [23] H. Ajiki, T. Ando, *J. Phys. Soc. Jpn.* 65 (1996) 505.
- [24] L. C. Venema, J. W. G. Wildöer, S. J. Tans, J. W. Janssen, L. J. Hinne, T. Tuinstra, L. P. Kouwenhoven, C. Dekker, *Science* 283 (1999) 52.
- [25] R. Kubo, *J. Phys. Soc. Jpn.* 12 (1957) 570.
- [26] U. Brandt, M. Moraweck, *J. Phys. C: Solid State Phys.* 15 (1982) 5255.
- [27] H. Shima, T. Nakayama, *Phys. Rev. B* 60 (1999) 14066.
- [28] H. Shima, T. Nomura, T. Nakayama, *Phys. Rev. B* 70 (2004) 075116.
- [29] Y. Umeno, T. Kitamura, A. Kushinma, *Comp. Materi. Sci.* 30 (2004) 283.